Proceedings of the Canadian Society for Mechanical Engineering International Congress 2022
CSME Congress 2022
June 5-8, 2022, Edmonton, AB, Canada

INTERACTION BETWEEN A SCREW DISLOCATION AND A MULTI-LAYERED COATED PIEZOELECTRIC INCLUSION

K.Q. Hu[1*], C.-F. Gao[1], Z.T. Chen[2], W.L. Yang[2], J.W. Fu[3]
[1]State Key Laboratory of Mechanics and Control of Mechanical Structures, Nanjing University of Aeronautics and Astronautics, Nanjing, Jiangsu, China
[2]Department of Mechanical Engineering, University of Alberta, Edmonton, AB, Canada
[3]Department of Mechanical Engineering, Nanjing University of Science and Technology, Nanjing, Jiangsu, China
*Corresponding author, Email: keqiang@nuaa.edu.cn

Abstract — The current study investigates the interaction of a piezoelectric dislocation with a multi-layered coated fiber inhomogeneity embedded in an infinite piezoelectric solid. In our study, three dissimilar material phases are involved: the matrix, the inclusion and the multi-layered coating layers. By applying the complex variable method and the series expansion technique, close-form solution for the stress field and electric field due to a piezoelectric screw dislocation near the coated inclusion is obtained. The image force acting on the screw dislocation is determined by using the generalized Peach-Koehler formula. A positive value of the image force indicates that the coated inclusion repels the dislocation, and a negative one implies that the dislocation is attracted by the coated inclusion. Finally, the influence of material properties and geometric size of the coating layers on the screw dislocation has been examined and discussed.

Keywords- piezoelectric composite material; multi-layered coated inclusion; screw dislocation; image force

I. INTRODUCTION

Because of the intrinsic electromechanical coupling effect, piezoelectric materials have been widely used in sensors, actuators and transducers for a variety of applications. Various types of defects embedded in piezoelectric materials, such as cracks, dislocations, cavities, and inclusions, can adversely influence the performance of the piezoelectric devices. Due to the brittleness and low fracture toughness of piezoelectric materials, fracture and damage analysis of piezoelectric materials has drawn considerable attention [1]. Investigation on the electro-elastic interaction of dislocation and inclusion is thus significant in studying the electric-mechanical behavior of piezoelectric components.

Deeg [2] considered the electro-elastic field of piezoelectric media with inclusions, and investigated the effect of a dislocation, a crack and an inclusion on the coupled response of piezoelectric solids. Ru and Schiavone [3] studied the anti-plane shear problem of an elliptic inclusion embedded in an infinite, isotropic, elastic medium, subjected to a uniform stress field, and proved that the state of deformation in the inclusion is a simple shear if and only if the curve enclosing the inclusion is an ellipse. By using the complex variable method, Wu et al. [4] derived the electro-elastic field of an infinite homogeneous piezoelectric medium with two piezoelectric circular cylindrical inclusions. Pak [5] studied the problem of a screw dislocation in a piezoelectric solid subjected to extend loads, obtained closed form solution and derived the generalized Peach-Koehler forces acting on the dislocation. The interaction between a screw dislocation and an elliptical piezoelectric inhomogeneity has been investigated [6]. Huang and Kuang [7] applied Green function to give out the generalized electro-mechanical force when the dislocation is located inside, outside and on the interface of an elliptical piezoelectric inhomogeneity in an infinite piezoelectric medium. The problem of a screw dislocation interacting with a coated inclusion embedded in an infinite solid was solved by Xiao et al. [8] by using the method of complex variable and series expansion technique.

In the current study, the interaction between a screw dislocation and a multi-layered coated piezoelectric inclusion is investigated. The three kinds of material phases involved in the problem are: the matrix, the fiber inclusion and the multi-layered coatings. All these three kinds of material phases are assumed to be piezoelectric and with different material properties. An analytical solution for the stress field due to a screw dislocation located in the matrix, inclusion and coating layers has been derived. The image force acting on the screw dislocation is calculated by using the generalized Peach-Koehler formula. The influence of the material properties of the coating layers on the dislocation is examined and discussed. The multi-layered coating model developed in this paper may be used to study the functionally graded materials (FGMs).

II. PROBLEM STATEMENT

The physical problem considered in this work is shown in Fig. 1, in which a circular piezoelectric inclusion with multi-layered coatings is embedded in an infinite piezoelectric material. A generalized screw dislocation is located at the point (e,0), $e > b$. It is noted that b_ϕ is the electro-potential dislocation and b_z is the screw dislocation. The materials occupy the regions, I, M and $k = 1,2,...,n$, respectively, correspond to the inclusion, the matrix and the k-th coating layer. All the phases are assumed to have the same material orientation poled along the z-direction with an isotropic Oxy-plane.

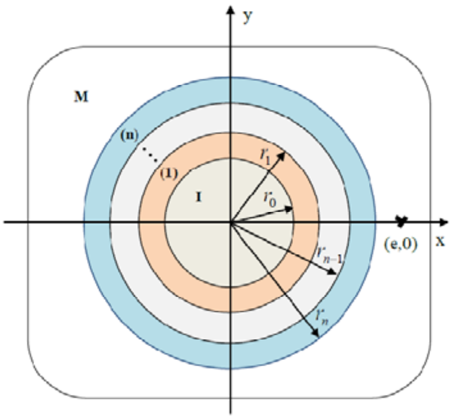

Figure 1. A multi-layered coated piezoelectric inclusion in an infinite matrix.

For the current boundary value problem, the deformation involved is independent of the spatial variable z, i.e., only the non-vanishing antiplane displacement and inplane electric fields are considered:

$$
\begin{aligned}
&u_x = u_y = 0, \ u_z = u_z(x, y) \\
&\phi = \phi(x, y)
\end{aligned} \tag{1}
$$

where u_z is the component of the displacement vector and ϕ is the electric potential.

According to the elasticity theory and considering the piezoelectric effect, the constitutive relations for the present antiplane problem are

$$
\begin{aligned}
&\sigma_{zx} = 2C_{44}\varepsilon_{xz} - e_{15}E_x, \ \sigma_{zy} = 2C_{44}\varepsilon_{yz} - e_{15}E_y \\
&D_x = 2e_{15}\varepsilon_{zx} + \lambda_{11}E_x, \ D_y = 2e_{15}\varepsilon_{zy} + \lambda_{11}E_y
\end{aligned} \tag{2}
$$

where C_{44} is the elastic constant, e_{15} is the piezoelectric coefficients and λ_{11} is the dielectric permittivity. σ_{ij} and ε_{ij} are the stresses and strains, respectively; D_j and E_j are the electric displacement and electric field, respectively. The subscripts stand for the coordinate x or y or z.

The governing equations for the anti-plane problem of the piezoelectric materials can be obtained as

$$
\begin{aligned}
&C_{44}\nabla^2 u_z + e_{15}\nabla^2\phi = 0 \\
&e_{15}\nabla^2 u_z - \lambda_{11}\nabla^2\phi = 0
\end{aligned} \tag{3}
$$

where $\nabla^2 = \partial^2/\partial x^2 + \partial^2/\partial y^2$ is the two-dimensional Laplacian operator in the variables x and y, u_z is the out-of-plane displacement and ϕ is the electric potential.

From (3), it can be seen that u_z and ϕ satisfy the Laplacian equation, so the solution of u_z and ϕ can be expressed as the real parts of the analytic functions $U(z)$ and $\Phi(z)$ as:

$$
\begin{aligned}
&u_z = \left[U(z) + \overline{U(z)}\right]/2 \\
&\phi = \left[\Phi(z) + \overline{\Phi(z)}\right]/2
\end{aligned} \tag{4}
$$

where z is the complex variable and the over-bar refers to the complex conjugate.

Following the procedure in [8], the holomorphic complex functions $U(z)$ and $\Phi(z)$ may be taken as

$$
\begin{aligned}
&U^I(z) = \frac{b_z}{2}\sum_{k=0}^{\infty}(a_{uk}^I + ib_{uk}^I)z^k \\
&\Phi^I(z) = \frac{b_\phi}{2}\sum_{k=0}^{\infty}(a_{\phi k}^I + ib_{\phi k}^I)z^k
\end{aligned} \tag{5}
$$

$$
\begin{aligned}
&U^{(j)}(z) = \frac{b_z}{2}\sum_{k=-\infty}^{\infty}(a_{uk}^{(j)} + ib_{uk}^{(j)})z^k \\
&\Phi^{(j)}(z) = \frac{b_\phi}{2}\sum_{k=-\infty}^{\infty}(a_{\phi k}^{(j)} + ib_{\phi k}^{(j)})z^k
\end{aligned} \tag{6}
$$

$$
\begin{aligned}
&U^M(z) = \frac{b_z}{2}\sum_{k=-\infty}^{-1}(a_{uk}^M + ib_{uk}^M)z^k - \frac{ib_z}{2\pi}\log(z-e) \\
&\Phi^M(z) = \frac{b_\phi}{2}\sum_{k=-\infty}^{-1}(a_{\phi k}^M + ib_{\phi k}^M)z^k - \frac{ib_\phi}{2\pi}\log(z-e)
\end{aligned} \tag{7}
$$

where the superscripts I and M denote the inclusion and the matrix, respectively, and the superscript *(j)* denotes the corresponding fields and variables of the *j*-th coating layer.

Assuming that the interfaces between the coating layers, the interface between the inclusion and coating layer (1), and the interface between the coating layer (n) and the matrix are all perfect, it implies that the normal components of the electric displacement and the tractions are continuous across the interfaces. The boundary conditions may be expressed as

$$
\begin{aligned}
&\sigma_{zr}^I = \sigma_{zr}^{(1)}, u_z^I = u_z^{(1)}, D_r^I = D_r^{(1)}, \phi^I = \phi^{(1)} \text{ on } \mathrm{L}_0 \\
&\sigma_{zr}^{(n)} = \sigma_{zr}^M, u_z^{(n)} = u_z^M, D_r^{(n)} = D_r^M, \phi^{(n)} = \phi^M \text{ on } \mathrm{L}_\mathrm{n} \\
&\sigma_{zr}^{(j)} = \sigma_{zr}^{(j+1)}, u_z^{(j)} = u_z^{(j+1)}, D_r^{(j)} = D_r^{(j+1)}, \phi^{(j)} = \phi^{(j+1)}
\end{aligned} \tag{8}
$$

where the interfaces L_j $(j = 0,1,...,n)$ denotes the circular planes $r_0 = a$, r_1, $r_2,...,r_n = b$, respectively.

The substitution of the complex functions $U(z)$ and $\Phi(z)$ into the constitutive equations leads to the components of the stresses and electric displacements, and the detailed expressions are omitted here.

Writing $z = r[\cos(\theta) + i\sin(\theta)]$, and applying the continuity boundary conditions, by comparing the coefficients of $\sin(k\theta)$ and $\cos(k\theta)$, we obtain linear equations to determine all the coefficients of the complex functions in (5-7).

The solutions can be obtained as

$$\begin{aligned} a_{uk}^{I} &= a_{\phi k}^{I} = a_{uk}^{(1)} = a_{\phi k}^{(1)} = a_{u(-k)}^{(1)} \\ &= a_{\phi(-k)}^{(1)} = a_{u(-k)}^{M} = a_{\phi(-k)}^{M} = 0 \end{aligned} \qquad (k \neq 0) \tag{9}$$

$$\begin{Bmatrix} a_{u0}^{I} \\ a_{\phi 0}^{I} \end{Bmatrix} = \begin{Bmatrix} a_{u0}^{(1)} \\ a_{\phi 0}^{(1)} \end{Bmatrix} \cdots = \begin{Bmatrix} a_{u0}^{(n)} \\ a_{\phi 0}^{(n)} \end{Bmatrix} = \begin{Bmatrix} \pi \\ \pi \end{Bmatrix} \tag{10}$$

$$\begin{Bmatrix} b_{uk}^{I} \\ b_{\phi k}^{I} \\ b_{u(-k)}^{M} \\ b_{\phi(-k)}^{M} \end{Bmatrix} = \frac{1}{ke^{k}} [\mathbf{E}]^{-1} \begin{Bmatrix} 1 \\ 1 \\ C_{44}^{M} b_z + e_{15}^{M} b\phi \\ e_{15}^{M} b_z - \lambda_{11}^{M} b\phi \end{Bmatrix} \tag{11}$$

$$\begin{Bmatrix} b_{uk}^{(1)} \\ b_{\phi k}^{(1)} \\ b_{u(-k)}^{(1)} \\ b_{\phi(-k)}^{(1)} \end{Bmatrix} = [\mathbf{A_2}]^{-1} [\mathbf{A_1}] \begin{Bmatrix} b_{uk}^{I} \\ b_{\phi k}^{I} \end{Bmatrix} \tag{12}$$

It is noted that the coefficients of the (j+1)-th layer and those of the j-th layer are related to each other which can be obtained by applying the transfer matrix method

$$\begin{aligned} \begin{Bmatrix} b_{uk}^{(j+1)} \\ b_{\phi k}^{(j+1)} \\ b_{u(-k)}^{(j+1)} \\ b_{\phi(-k)}^{(j+1)} \end{Bmatrix} &= \left[\mathbf{M}_b^{(j)}\right] \begin{Bmatrix} b_{uk}^{(j)} \\ b_{\phi k}^{(j)} \\ b_{u(-k)}^{(j)} \\ b_{\phi(-k)}^{(j)} \end{Bmatrix} \\ &= \begin{bmatrix} \left[\mathbf{B}_1^{(j)}\right] & \frac{1}{r_j^{2k}} \left[\mathbf{B}_2^{(j)}\right] \\ r_j^{2k} \left[\mathbf{B}_2^{(j)}\right] & \left[\mathbf{B}_1^{(j)}\right] \end{bmatrix} \begin{Bmatrix} b_{uk}^{(j)} \\ b_{\phi k}^{(j)} \\ b_{u(-k)}^{(j)} \\ b_{\phi(-k)}^{(j)} \end{Bmatrix} \end{aligned} \tag{13}$$

where r_j is the outer radius of the j-th coating layer and the matrices $[\mathbf{A_1}]$, $[\mathbf{A_2}]$ $\left[\mathbf{B}_1^{(j)}\right]$, $\left[\mathbf{B}_2^{(j)}\right]$, and $[\mathbf{E}]$ are related to the material properties, the geometric sizes and the loading conditions. The detailed expressions of these matrices are defined as

$$[\mathbf{A}_1] = \begin{bmatrix} 1 & 0 \\ 0 & 1 \\ C_{44}^{I} b_z & e_{15}^{I} b_\phi \\ e_{15}^{I} b_z & -\lambda_{11}^{I} b_\phi \end{bmatrix} \tag{14}$$

$$[\mathbf{A}_2] = \begin{bmatrix} 1 & -1/a^{2k} & 0 & 0 \\ 0 & 0 & 1 & -1/a^{2k} \\ C_{44}^{(1)} b_z & C_{44}^{(1)} b_z / a^{2k} & e_{15}^{(1)} b_\phi & e_{15}^{(1)} b_\phi / a^{2k} \\ e_{15}^{(1)} b_z & e_{15}^{(1)} b_z / a^{2k} & -\lambda_{11}^{(1)} b_\phi & -\lambda_{11}^{(1)} b_\phi / a^{2k} \end{bmatrix} \tag{15}$$

$$\begin{aligned} \left[\mathbf{B}_1^{(j)}\right] &= \frac{1}{2} \left[\left[\mathbf{C}^{(j+1)}\right]^{-1} \left[\mathbf{C}^{(j)}\right] + [\mathbf{I}]\right] \\ \left[\mathbf{B}_2^{(j)}\right] &= \frac{1}{2} \left[\left[\mathbf{C}^{(j+1)}\right]^{-1} \left[\mathbf{C}^{(j)}\right] - [\mathbf{I}]\right] \end{aligned} \tag{16}$$

$$\begin{aligned} \left[\mathbf{C}^{(j)}\right] &= \begin{bmatrix} C_{44}^{(j)} b_z & e_{15}^{(j)} b_\phi \\ e_{15}^{(j)} b_z & -\lambda_{11}^{(j)} b_\phi \end{bmatrix} \\ \left[\mathbf{C}^{(j+1)}\right] &= \begin{bmatrix} C_{44}^{(j+1)} b_z & e_{15}^{(j+1)} b_\phi \\ e_{15}^{(j+1)} b_z & -\lambda_{11}^{(j+1)} b_\phi \end{bmatrix} \end{aligned} \tag{17}$$

$$\begin{aligned} [\mathbf{E}] &= [[\mathbf{E}_1] \quad [\mathbf{E}_2]] \\ [\mathbf{E}_1] &= [\mathbf{B}][\mathbf{A}_2]^{-1}[\mathbf{A}_1] \\ [\mathbf{E}_2] &= -\frac{1}{b^{2k}} \begin{bmatrix} -1 & 0 \\ 0 & -1 \\ C_{44}^{M} b_z & e_{15}^{M} b_\phi \\ e_{15}^{M} b_z & -\lambda_{11}^{M} b_\phi \end{bmatrix} \end{aligned} \tag{18}$$

$$[\mathbf{B}] = \begin{bmatrix} X_{11} & X_{13} & X_{12} & X_{14} \\ X_{21} & X_{23} & X_{22} & X_{24} \\ Y_{11} & Y_{13} & Y_{12} & Y_{14} \\ Y_{21} & Y_{23} & Y_{22} & Y_{24} \end{bmatrix} \tag{19}$$

$$\begin{aligned} X_{1j} &= V_{1j} - \frac{V_{3j}}{b^{2k}}, \quad X_{2j} = V_{2j} - \frac{V_{4j}}{b^{2k}} \\ [\mathbf{Y}] &= \begin{bmatrix} Y_{11} & Y_{12} & Y_{13} & Y_{14} \\ Y_{21} & Y_{22} & Y_{23} & Y_{24} \end{bmatrix} \\ &= \begin{bmatrix} C_{44}^{(n)} b_z & e_{15}^{(n)} b_\phi & \frac{C_{44}^{(n)} b_z}{b^{2k}} & \frac{e_{15}^{(n)} b_\phi}{b^{2k}} \\ e_{15}^{(n)} b_z & -\lambda_{11}^{(n)} b_\phi & \frac{e_{15}^{(n)} b_z}{b^{2k}} & -\frac{\lambda_{11}^{(n)} b_\phi}{b^{2k}} \end{bmatrix} [\mathbf{V}] \end{aligned} \tag{20}$$

$$\begin{aligned} [\mathbf{V}] &= \prod_{j=1}^{n-1} \left[\mathbf{M}_b^{(j)}\right] \\ &= \left[\mathbf{M}_b^{(n-1)}\right]\left[\mathbf{M}_b^{(n-2)}\right] \cdots \left[\mathbf{M}_b^{(2)}\right]\left[\mathbf{M}_b^{(1)}\right] \\ &= \begin{bmatrix} V_{11} & V_{12} & V_{13} & V_{14} \\ V_{21} & V_{22} & V_{23} & V_{24} \\ V_{31} & V_{32} & V_{33} & V_{34} \\ V_{41} & V_{42} & V_{43} & V_{44} \end{bmatrix} \end{aligned} \tag{21}$$

III. CLOSED FORM SOLUTIONS

By substituting (5-7) into (4) and (2), the field components in the circular cylindrical inclusion, the coating layers and the matrix can be obtained. The closed form solutions of the shear stresses and the electric displacements inside the inclusion and the matrix can be given as follows

$$
\begin{aligned}
\sigma_{zx}^{I} &= -\frac{1}{2\pi}\sum_{k=1}^{\infty} kr^{k}\left[C_{44}^{I} b_z b_{uk}^{I} + e_{15}^{I} b_\phi b_{\phi k}^{I}\right]\sin(k-1)\theta \\
\sigma_{zy}^{I} &= -\frac{1}{2\pi}\sum_{k=1}^{\infty} kr^{k}\left[C_{44}^{I} b_z b_{uk}^{I} + e_{15}^{I} b_\phi b_{\phi k}^{I}\right]\cos(k-1)\theta
\end{aligned} \tag{22}
$$

$$
\begin{aligned}
D_{x}^{I} &= -\frac{1}{2\pi}\sum_{k=1}^{\infty} kr^{k}\left[e_{15}^{I} b_z b_{uk}^{I} - \lambda_{11}^{I} b_\phi b_{\phi k}^{I}\right]\sin(k-1)\theta \\
D_{y}^{I} &= -\frac{1}{2\pi}\sum_{k=1}^{\infty} kr^{k}\left[e_{15}^{I} b_z b_{uk}^{I} - \lambda_{11}^{I} b_\phi b_{\phi k}^{I}\right]\cos(k-1)\theta
\end{aligned} \tag{23}
$$

$$
D_{x}^{M} = -\frac{1}{2\pi}\left\{\begin{aligned}
& e_{15}^{M} b_z \left[\begin{aligned} &\sum_{k=1}^{\infty} kr^{-k-1} b_{u(-k)}^{M}\sin(k+1)\theta \\ &+ \frac{y}{(x-e)^2+y^2}\end{aligned}\right] \\
& -\lambda_{11}^{M} b_\phi \left[\begin{aligned} &\sum_{k=1}^{\infty} kr^{-k-1} b_{\phi(-k)}^{M}\sin(k+1)\theta \\ &+ \frac{y}{(x-e)^2+y^2}\end{aligned}\right]
\end{aligned}\right\} \tag{24}
$$

$$
D_{y}^{M} = \frac{1}{2\pi}\left\{\begin{aligned}
& e_{15}^{M} b_z \left[\begin{aligned} &\sum_{k=1}^{\infty} kr^{-k-1} b_{u(-k)}^{M}\cos(k+1)\theta \\ &+ \frac{x-e}{(x-e)^2+y^2}\end{aligned}\right] \\
& -\lambda_{11}^{M} b_\phi \left[\begin{aligned} &\sum_{k=1}^{\infty} kr^{-k-1} b_{\phi(-k)}^{M}\cos(k+1)\theta \\ &+ \frac{x-e}{(x-e)^2+y^2}\end{aligned}\right]
\end{aligned}\right\} \tag{25}
$$

The corresponding solutions of the shear stresses and the electric displacements inside the coating layers can be easily obtained in a similar manner and detailed expressions are omitted.

It is noted that when there is only one coating layer, i.e., $n=1$, the solutions obtained is the same as the result of [8]. When the number is big enough, the current model can be used to simulate the functionally graded coating.

IV. Image Force

It is of great interests to study the image force acting on the dislocation when the dislocation problems are discussed. Following Pak [5], the generalized Peach-Koehler forces acting on a screw dislocation can be expressed as

$$
\begin{aligned}
F_x &= b_z \sigma_{zy}^{T} + b_\phi D_y^{T} \\
F_y &= -b_z \sigma_{zx}^{T} - b_\phi D_x^{T}
\end{aligned} \tag{26}
$$

where the variables σ_{zx}^{T}, σ_{zy}^{T}, D_x^{T} and D_y^{T} can be obtained by subtracting the corresponding fields generated by the dislocation in a homogeneous matrix.

When the dislocation is located at the point $(e,0)$, the expression of σ_{zx}^{T}, σ_{zy}^{T}, D_x^{T} and D_y^{T} can be given as

$$\sigma_{zx}^{T} = 0 \tag{27}$$

$$\sigma_{zy}^{T} = \frac{1}{2\pi}\left[C_{44}^{M} b_z \sum_{k=1}^{\infty} kr^{-k-1} b_{u(-k)}^{M} + e_{15}^{M} b_\phi \sum_{k=1}^{\infty} kr^{-k-1} b_{\phi(-k)}^{M}\right] \tag{28}$$

$$D_x^{T} = 0 \tag{29}$$

$$D_y^{T} = \frac{1}{2\pi}\left[e_{15}^{M} b_z \sum_{k=1}^{\infty} kr^{-k-1} b_{u(-k)}^{M} - \lambda_{11}^{M} b_\phi \sum_{k=1}^{\infty} kr^{-k-1} b_{\phi(-k)}^{M}\right] \tag{30}$$

Substitution of (27-30) into (26) leads to the expressions of the image forces as

$$
\begin{aligned}
F_x &= \frac{1}{2\pi}\sum_{k=1}^{\infty} ke^{-k-1}\left[\begin{aligned} &(C_{44}^{M} b_z^2 + e_{15}^{M} b_z b_\phi) b_{u(-k)}^{M} \\ &+ (e_{15}^{M} b_z b_\phi - \lambda_{11}^{M} b_\phi^2) b_{\phi(-k)}^{M}\end{aligned}\right] \\
F_y &= 0
\end{aligned} \tag{31}
$$

V. Examples And Discussions

In this section, some examples are given to illustrate the application of the closed form solutions obtained in previous sections. The screw dislocation is assumed to be located at the point ($e,0$), and the screw dislocation and electro-potential dislocation are assumed to be $b_z = 1\times 10^{-9}\,\mathrm{m}$ and $b_\phi = 1\mathrm{V}$, respectively.

To study the image force more explicitly, we allow the dislocations to have only one nonzero strength characteristic, i.e., either b_z or b_ϕ. The following normalizing factors are introduced respectively for the case $b_z = 1\times 10^{-9}\mathrm{m}$, $b_\phi = 0$ and $b_\phi = 1\mathrm{V}$, $b_z = 0$, respectively

$$F_{bz0} = \frac{C_{44}^{M} b_z^2}{2\pi b},\quad F_{b\phi 0} = \frac{\lambda_{11}^{M} b_\phi^2}{2\pi b} \tag{32}$$

Assume that the material properties of the j -th layer coating are ρ_{j} times of the material properties of the inclusion, i.e.,

$$\left[\mathbf{C}^{(j)}\right] = \begin{bmatrix} C_{44}^{(j)} & e_{15}^{(j)} \\ e_{15}^{(j)} & -\lambda_{11}^{(j)} \end{bmatrix} = \rho_j \begin{bmatrix} C_{44}^{I} & e_{15}^{I} \\ e_{15}^{I} & -\lambda_{11}^{I} \end{bmatrix} \tag{33}$$

In the following calculations, it is assumed that the material properties of the matrix is two times of those of the inclusion, i.e.,

$$\left[\mathbf{C}^{M}\right]=\begin{bmatrix} C_{44}^{M} & e_{15}^{M} \\ e_{15}^{M} & -\lambda_{11}^{M} \end{bmatrix}=2\begin{bmatrix} C_{44}^{I} & e_{15}^{I} \\ e_{15}^{I} & -\lambda_{11}^{I} \end{bmatrix} \tag{34}$$

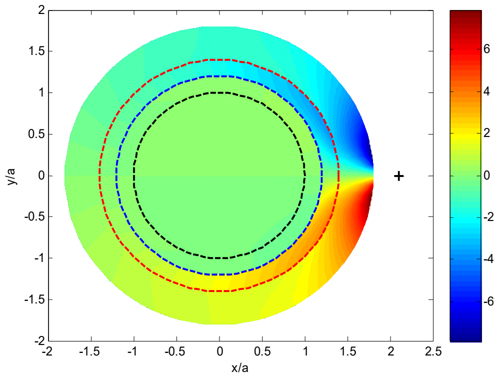

Figure 2. Normalized shear stress σ_{zx}/σ_0 in the coated piezoelectric composite when $b_\phi = 1\text{V}$, $\rho_1 = 0.5$, $\rho_2 = 4$, $\rho_M = 2$.

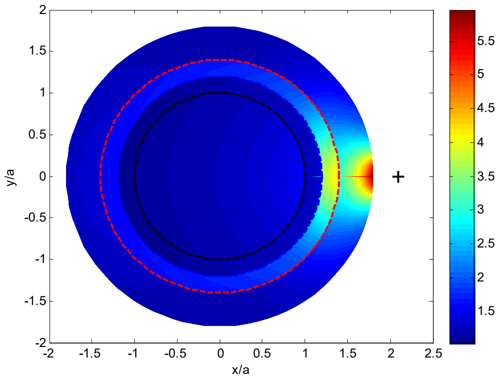

Figure 3. Normalized shear stress σ_{zy}/σ_0 in the coated piezoelectric composite when $b_\phi = 1\text{V}$, $\rho_1 = 0.5$, $\rho_2 = 4$, $\rho_M = 2$.

Fig. 2 and Fig. 3 show the normalized shear stresses σ_{zx}/σ_0 and σ_{zy}/σ_0 when the electro-potential dislocation $b_\phi = 1\text{V}$ ($b_z = 0$) is applied at the point ($e,0$), $r_2 = b = 1.4a$, $e = 1.5b$. The value of σ_0 is defined as

$$\sigma_0 = -\frac{1}{2\pi}\sum_{k=1}^{\infty} k\left(C_{44}^{I} b_z b_{uk}^{I} + e_{15}^{I} b_\phi b_{\phi k}^{I}\right) \tag{35}$$

which is the value of the shear stress of $\sigma_{zy}^{I}(r,\theta)$ when $r/a = 1$ and $\theta = 0$. The material properties of the composite is characterized as $\rho_1 = 0.5$, $\rho_2 = 4$, $\rho_M = 2$.

The dotted lines denote the interfaces between different phases. It is observed that the shear stresses and across the interfaces are discontinuous (except at some special points), and the magnitude of the stresses in coating layers are dependent on the material properties of the coating layers and the value of the dislocation. As the dislocation b_ϕ is located on the x-axis, the shear stress σ_{zx} is anti-symmetric about the x-axis and the shear stress σ_{zy} is symmetric about the x-axis.

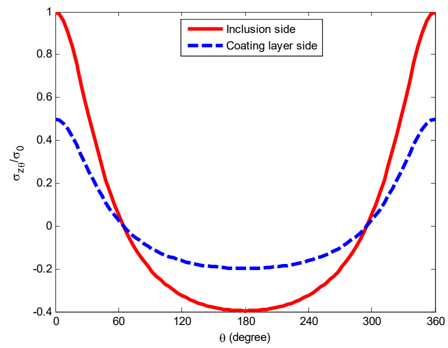

Figure 4. Normalized hoop stress $\sigma_{z\theta}/\sigma_0$ on the interface between inclusion and coating when $b_\phi = 1\text{V}$.

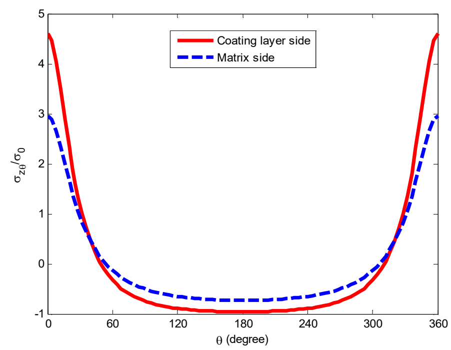

Figure 5. Normalized hoop stress $\sigma_{z\theta}/\sigma_0$ on the interface between matrix and coating when $b_\phi = 1\text{V}$.

The normalized hoop stresses $\sigma_{z\theta}/\sigma_0$ on the interface between the inclusion and the coating layer are displayed in Fig. 4 versus the angle θ when $b_\phi = 1\text{V}$ ($b_z = 0$). Fig. 5 shows the angular variation of the normalized hoop stresses $\sigma_{z\theta}/\sigma_0$ on the interface between the matrix and the coating layer. It is observed that the hoop stresses on the interface are not continuous at the contact point, except for the two particular angles. The maximum magnitude of the hoop stresses on the coating layer side is larger than that on the inclusion or matrix side for the current composite material combination $\rho_1 = 0.5,\ \rho_2 = 4,\ \rho_M = 2$.

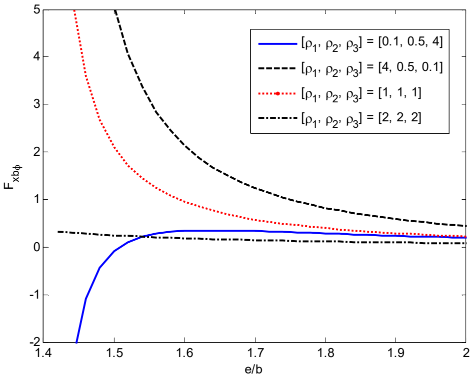

Figure 6. Normalized image force $F_{xb\phi}$ versus the distance e/b.

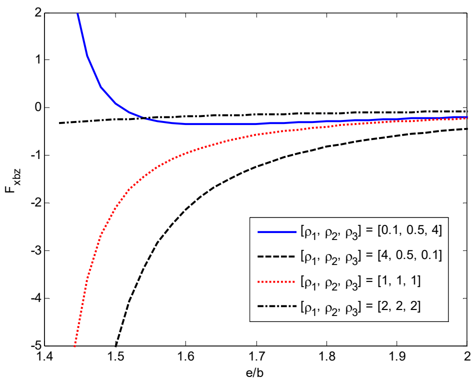

Figure 7. Normalized image force F_{xbz} versus the distance e/b.

The influence of the distance on the image forces $F_{xb\phi}$ and F_{xbz} are displayed in Fig. 6 and Fig. 7, respectively. It is noted that a positive value of the image force indicates that the coated inclusion repels the dislocation, while a negative value of the image force implies that the dislocation is attracted by the coated inclusion. It is seen from Fig. 6 that when the three coating layers have the material properties as $\rho_1 = 0.1,\ \rho_2 = 0.5,\ \rho_3 = 4$, when the distance e increases, the image force $F_{xb\phi}$ increases from negative value to a positive maximum, and then decreases to a minimum of positive value. It implies that the dislocation is attracted by the inclusion when e is small and it is repelled when e is big. The other three material property combinations indicate that the dislocation is repelled by the coated inclusion. Fig. 7 displays a totally contrary trend of the image force F_{xbz} when the distance e increases.

VI. Conclusion

A closed-form analytical solution is obtained for a piezoelectric screw dislocation interacting with multi-layered coated inclusion by using the complex variable method. The results indicate that the coating layers play an important role in the problem of the interaction between dislocation and inclusion. The analytical solution obtained can be used as Green functions to solve related inclusion-crack interaction problems in piezoelectric composites.

Acknowledgment

This work is supported by National Natural Science Foundation of China for Creative Research Groups (Grant No. 51921003) and the Joint Fund of Advanced Aerospace Manufacturing Technology Research (Grant No. U1937601).

References

[1] K. Q. Hu, Z. T. Chen, "Size effect on crack kinking in a piezoelectric strip under impact loading," Mech. Mater. vol. 61, pp. 60-72, 2013.

[2] W. F. Deeg, The analysis of dislocation, crack, and inclusion problems in piezoelectric solids. Ph.D. thesis, Stanford University, Stanford, CA: 1980.

[3] C. –Q. Ru, P. Schiavone, "On the elliptic inclusion in anti-plane shear," Mathe. Mech. Solids, vol. 1, pp. 327-333, 1996.

[4] L. Z. Wu, J. Chen, and Q. G. Meng, "Two piezoelectric circular cylindrical inclusions in the infinite piezoelectric medium," Int. J. Eng. Sci. vol. 38, pp. 879-892, 2000.

[5] Y. E. Pak, "Force on a piezoelectric dislocation," ASME J. Appl. Mech. vol. 57, pp. 863-869, 1990.

[6] W. Deng, S. A. Meguid, "Analysis of a screw dislocation inside an elliptical inhomogeneity in piezoelectric solids," Int. J. Solids Struct. vol. 36, pp. 1449-1469, 1999.

[7] Z. Huang, Z. B. Kuang, "Dislocation inside a piezoelectric media with an elliptic inhomogeneity," Int. J. Solids Struct. vol. 38, pp. 8456-8479, 2001.

[8] Z. M. Xiao, J. Yan, and B. J. Chen, "Electro-elastic stress analysis for a screw dislocation interacting with a coated inclusion in a piezoelectric solid," Acta Mech. vol. 172, pp. 237-249, 2004.